Controlling interlayer diffusion to achieve sustained, multiagent delivery from layer-by-layer thin films

Kris C. Wood*, Helen F. Chuang*, Robert D. Batten*, David M. Lynn†, and Paula T. Hammond*‡

*Department of Chemical Engineering, Massachusetts Institute of Technology, 77 Massachusetts Avenue, Room 66-546, Cambridge, MA 02139; and †Department of Chemical and Biological Engineering, University of Wisconsin, 1415 Engineering Drive, Madison, WI 53706

Communicated by Robert Langer, Massachusetts Institute of Technology, Cambridge, MA, April 10, 2006 (received for review September 8, 2005)

We present the fabrication of conformal, hydrolytically degradable thin films capable of administering sustained, multiagent release profiles. Films are constructed one molecular layer at a time by using the layer-by-layer, directed-deposition technique; the subsequent hydrolytic surface erosion of these systems results in the release of incorporated materials in a sequence that reflects their relative positions in the film. The position of each species is determined by its ability to diffuse throughout the film architecture, and, as such, the major focus of this work is to define strategies that physically block interlayer diffusion during assembly to create multicomponent, stratified films. By using a series of radiolabeled polyelectrolytes as experimental probes, we show that covalently crosslinked barriers can effectively block interlayer diffusion, leading to compartmentalized structures, although even very large numbers of ionically crosslinked (degradable or nondegradable) barrier layers cannot block interlayer diffusion. By using these principles, we designed degradable films capable of extended release as well as both parallel and serial multiagent release. The ability to fabricate multicomponent thin films with nanoscale resolution may lead to a host of new materials and applications.

The ability to engineer surfaces that present multiple functionalities when and where they are needed could lead to important advances in electrooptical devices, separations, and biomaterials (1, 2). For example, in the area of drug delivery, there is a need for low-cost "smart" coatings that balance the ability to release complex drug profiles with the flexibility of incorporation into a range of biomaterials, including those with large area sizes or nonplanar geometries, such as pins, sutures, prosthetic bones, devices, and microparticles. The layer-by-layer (LbL) electrostatic assembly technique is ideally suited for such applications because it allows for absolute control over the order in which multiple functional elements are incorporated into a growing film (3). However, the development of truly stratified, multicompartment LbL films has been largely unsuccessful with many biomacromolecules because of the phenomenon of interlayer diffusion, which results in blended structures lacking regular, controlled order (4). In this work, we systematically probe a range of strategies designed to solve this problem by placing physical barriers between various components within a single film to control interlayer diffusion. We measure the effect of each type of barrier with a system consisting of a hydrolytically degradable polymer (Fig. 1, polymer 1) alternately deposited with a series of radiolabeled polyelectrolytes. Top-down film degradation results in the release of components in a sequence that reflects their relative positions in the film; thus, we can quantify the effects of various barrier strategies aimed at limiting diffusion behavior. With this approach, we uncover a set of strategies that allow for the production of compartmentalized films capable of passively releasing complex, tuned release profiles. In addition to uncovering fundamental strategies to control interlayer diffusion in LbL films, this work may lead to important applications in drug delivery by allowing for the fabrication of nanoscale materials coatings capable of releasing sustained, multidrug schedules from surfaces of virtually any composition or geometry under physiological conditions.

The LbL electrostatic assembly technique entails the sequential adsorption of monolayers of oppositely charged polymers, colloids, or other materials onto a solid substrate to form a cohesive, ionically crosslinked thin film (3). Multilayers can be deposited rapidly and inexpensively atop large area surfaces of any geometry while allowing for nanometer-scale control over a range of physical properties (3, 5). Furthermore, the all-aqueous processing of LbL systems allows for the incorporation of sensitive biomolecules, such as proteins and DNA (6–10). More broadly, the technique also can be extended to include any molecular species that is either charged or can be encapsulated in a charged "carrier" (i.e., dendrimer, micelle, chaperone, or nanoparticle), thus making it possible to incorporate a wide range of species without regard to molecular weight or intrinsic charge. On the basis of these attributes, we hypothesized that degradable LbL systems based on a hydrolytically degradable polyion, such as polymer 1, might be useful for a range of drug delivery applications, particularly those involving the release of complex schedules of drugs (11–13) (see Fig. 7, which is published as supporting information on the PNAS web site). However, although promising, this technology has been limited because of the inability to control the relative positions and distributions of multiple species residing within a single film, resulting in highly disorganized architectures (ref. 14 and K.C.W., D.M.L., and P.T.H., unpublished data). The phenomenon responsible for this lack of control is referred to as interlayer diffusion, the tendency of some species to diffuse throughout LbL systems during the deposition process. All polyelectrolytes fall into one of two broad classes with respect to interlayer diffusion: diffusing polyelectrolytes (i.e., many polypeptides and polysaccharides) are able to rapidly diffuse throughout LbL architectures during assembly, resulting in poorly organized, blended structures, whereas nondiffusing polyelectrolytes (i.e., most synthetic, strong polyelectrolytes) cannot, resulting in spatially organized structures wherein each deposited species is only able to interact with neighboring layers in close proximity (usually two to three layers) (4).

In this study, we examine the effects of various physical barrier strategies on both diffusing and nondiffusing systems by tracking the release of radiolabeled polyelectrolytes that exhibit either extensive diffusing behavior [heparin (HEP)] or nondiffusing behavior [dextran sulfate (DS)] when incorporated into LbL structures. We show that covalently crosslinked barriers deposited between the two labeled components can effectively block interlayer diffusion, leading to compartmentalized structures. In contrast, even very large numbers of ionically crosslinked (degradable or nondegradable) barrier layers cannot block inter-

Conflict of interest statement: No conflicts declared.

Abbreviations: FTIR, Fourier-transform infrared spectroscopy; LbL, layer-by-layer; DS, dextran sulfate; HEP, heparin; PDAC, poly(diallyldimethylammonium chloride); SPS, sulfonated poly(styrene); PAA, poly(acrylic acid); PAH, poly(allylamine hydrochloride).

‡To whom correspondence should be addressed. E-mail: hammond@mit.edu.

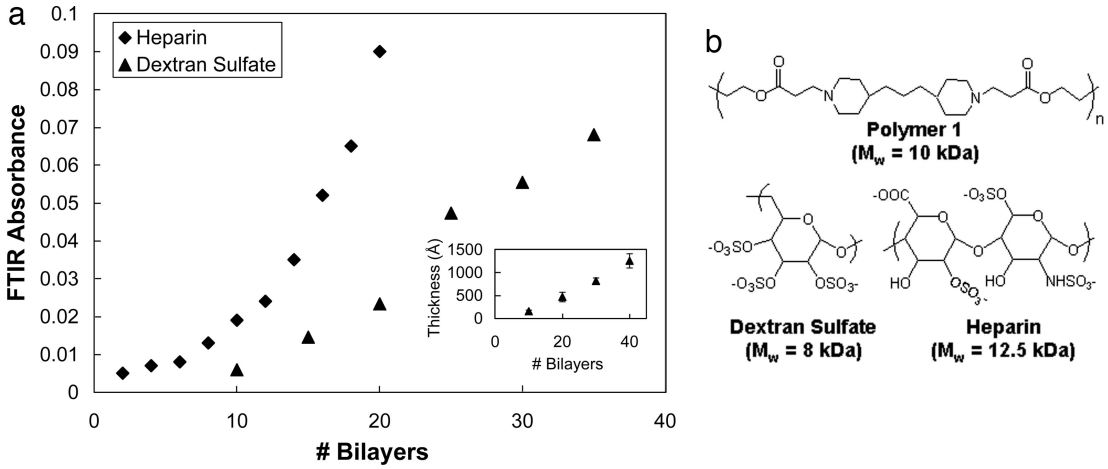

Fig. 1. Assembly of LbL films. (*a*) A plot of FTIR absorbance versus number of thin-film bilayers demonstrates LbL assembly of polymer 1/HEP (◆) and polymer 1/DS (▲) films exhibiting exponential and linear growth, respectively. (*Inset*) Thickness versus number of bilayers for polymer 1/DS films. (*b*) Chemical structures of degradable polymer and model drugs used in this study.

layer diffusion. By connecting interlayer diffusion with ultimate film architecture and release properties and by further studying the fabrication parameters that allow us to control interlayer diffusion, we uncovered a set of guiding principles that should significantly aid future attempts to build highly organized LbL structures. Furthermore, the demonstration that these films can release multiple agents either in parallel or in series may have important implications for drug delivery and controlled release materials.

Results and Discussion

Build Up and Release Properties of Single-Component Films. As a basis for these studies, we selected two radiolabeled polysaccharides, HEP and DS, which exhibit growth behavior associated with diffusive and nondiffusive species, respectively (4). Fig. 1*a* is a plot of the transmission mode Fourier-transform infrared spectroscopy (FTIR) absorbance recorded from films containing either polymer 1/Hep or polymer 1/DS. Specifically, the absorbances from sulfonic acid groups at 1,035 cm^{-1} (HEP) and 1,017 cm^{-1} (DS) were measured after the deposition of indicated bilayers. All measurements were taken from the same spot on the surface of the film in transmission mode on infrared-transparent, zinc selenide substrates. Fig. 1*a Inset* shows the film thickness versus number of deposited bilayers for a polymer 1/DS film. Both FTIR and ellipsometry demonstrate that the quantity of DS incorporated into the film is linearly proportional to the number of adsorption cycles, a commonly observed characteristic of many LbL systems. Linear build-up behavior is characteristic of films whose constituent polyions adsorb directly onto the film surface during each deposition step. Interlayer diffusion does not occur in these systems, which, as a result, form spatially organized structures wherein species deposited at a given step are able to interact only with neighboring species that are in close proximity (e.g., two to three layers) (3, 15, 16). In contrast, HEP-based films exhibit an exponential increase in absorbance with increasing numbers of adsorbed layers. Exponentially growing films, which are most commonly composed of hydrophilic polyelectrolytes or biologically derived materials (i.e., peptides and polysaccharides), are poorly organized blended architectures characterized by the complete "in" and "out" diffusion of adsorbing species throughout the growing film during the film's assembly process (4, 17–19). A series of recent studies offer mechanistic explanations (19, 20) and direct evidence (4) for this process, wherein a species deposited at a given step can reside in any position throughout the film.

Fig. 1*b* depicts the chemical structures of the repeat units of polymer 1, HEP, and DS, the three polymers used in this study. Polymer 1 is a cationic, degradable poly(β amino ester) synthesized by the conjugate addition-step polymerization of a diamine and a diacrylate; it represents one member of a library of >2,350 degradable poly(β amino esters) recently synthesized and screened for their abilities to deliver DNA to cells in culture (21). Both model drug compounds, HEP and DS, are polysaccharides that possess similar structural attributes, including strong (sulfonic) acid groups on each repeat unit and relatively low molecular weights.

To better understand the degradation and release behavior exhibited by the two model polyelectrolytes, we simultaneously measured release and degradation of single-component films containing each species. Fig. 2 shows degradation and release from 20 bilayer polymer 1/HEP and polymer 1/DS systems, respectively, after immersion in PBS buffer at pH 7.4. As previously documented, complete degradation and consequent release from polymer 1/HEP systems occurred within 20 h. Film thickness was observed to decrease linearly after a brief swelling period of 0.5–2.0 h upon first being exposed to aqueous solution (13). DS-based films exhibited similar degradation and release behavior, although with kinetics ≈5-fold slower than their HEP-based counterparts. The initial release observed in both cases within the first few hours of degradation likely reflects passive release from the surface, as the outermost layer of each film consists of the labeled compound. The fact that this effect is more pronounced in the case of HEP likely reflects the presence of interlayer diffusion, which results in a thick outer layer of diffusible material at the film surface (4). Interestingly, in both cases, film thickness was observed to decrease linearly with time; furthermore, the apparent roughness of the film surface, taken from the standard deviation in film thickness measured at 10 predetermined spots on the surface, was observed to remain constant, or even decrease, with time. Taken together, these data suggest top-down surface erosion of the films; one would anticipate that patchy or bulk degradation would result in a much larger standard deviation and nonlinear degradation behavior. [Recent atomic force microscopy investigations also provide further physical support to the mechanism of top-down degradation (11, 22).] Given the linear degradation and surface erosion observed in both sets of thin films, the vastly different kinetics of degradation and release exhibited by these two systems reflect differences in film organization, wherein the diffusive character of HEP contributes to loose gradient films

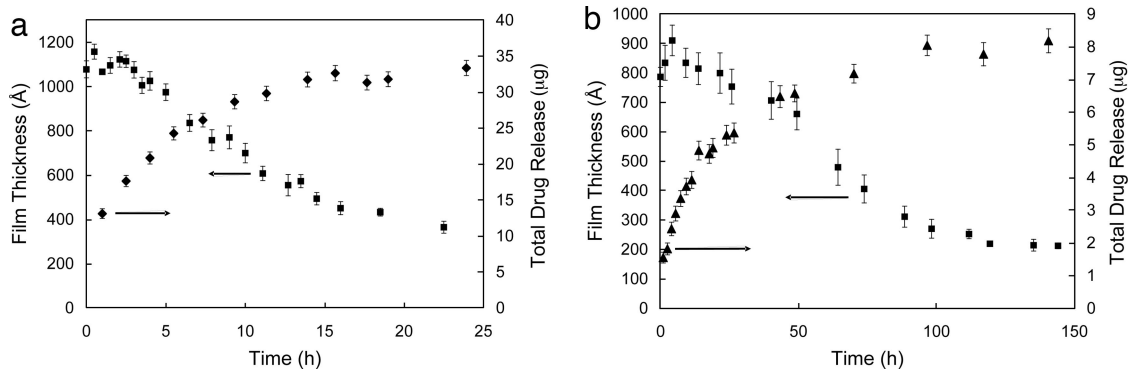

Fig. 2. Degradation (■) and drug release (▲) from single component films used in this study. (*a*) Twenty bilayer polymer 1/HEP films. (*b*) Twenty bilayer polymer 1/DS films.

with larger quantities of HEP in the top layers, compared with their relatively more stratified and more densely ion-crosslinked DS counterparts, which have a constant distribution of DS throughout the film.

To further verify that release occurs by means of surface erosion and to explore the relationship between interlayer diffusion and release properties of degradable LbL constructs, we constructed a series of 20, 50, and 80 bilayer films containing either polymer 1/HEP (Fig. 3*a*) or polymer 1/DS (Fig. 3*b*). For the case of polymer 1/HEP systems, the release behavior reflects intuition for the case of an exponentially growing system with top-down degradation behavior. The slope of the release curve differs dramatically between films of varying thickness, a reflection of the fact that exponentially growing systems result in the formation of disorganized films with increasing amounts of the diffusible species (HEP) at each deposition step (initial release rates of 0.4, 3.7, and 7.9 $\mu g \cdot cm^{-2} \cdot h^{-1}$ were observed for 20, 50, and 80 bilayer films, respectively). Moreover, each HEP-based system was observed to release its contents rapidly (in <20 h) without regard to its thickness, again a likely reflection of the fact that the majority of the model polyelectrolyte is contained in the upper layers after multiple deposition cycles (4). In sharp contrast, release from polymer 1/DS films of increasing thickness results in all cases in an initial phase of linear release followed by a "leveling off" as degradation is completed. Interestingly, as might be expected for the case of top-down release from a series of linearly growing films, we observed that all three films released DS at a relatively equivalent rate during the linear release phase (release rates of 0.07, 0.06, and 0.08 $\mu g \cdot cm^{-2} \cdot h^{-1}$ were observed for 20, 50, and 80 bilayer films, respectively) and that the duration of this linear release phase was proportional to the number of deposited bilayers (20, 49, and 97 h for 20, 50, and 80 bilayer films, respectively). The slow release kinetics of these systems likely reflects the higher effective ionic crosslink density of the thin films and much lower interlayer diffusivity of the model polyelectrolyte within the multilayer matrix. Importantly, these data suggest that the hydrolytic degradation of LbL systems can provide quantitative insights into the architecture and organization of these films. Moreover, this demonstration suggests that the duration of time over which release occurs can be broadly tuned in linearly growing (nondiffusing) systems simply by changing the number of deposited layers.

Controlling Interlayer Diffusion to Modulate Multiagent Release Profiles. Having demonstrated the ability of hydrolytically degradable LbL thin films to act as a probe to gain quantitative insight into film organization and architecture, we next sought to evaluate a range of strategies to control the relative positions of multiple, labeled species within a single film by constructing physical barriers to separate the two components. We constructed films first containing 20–40 base layers of polymer 1/HEP, followed by a set of "barrier" layers consisting of either polymer 1/sulfonated poly(styrene) (SPS) (degradable), poly(diallyldimethylammonium chloride) (PDAC)/SPS (nondegradable), thermally crosslinked poly(allylamine hydrochloride) (PAH)/poly(acrylic acid) (PAA), or nothing at all. Finally, we constructed a set of 20–40 surface layers of polymer 1/DS. In a similar fashion, we also constructed films identical to the others, except that the order of the labeled components was reversed (DS base layers and HEP surface layers) (see Fig. 4).

As shown in Fig. 5, when a base layer of polymer 1/DS was coated with a single bilayer of PAH/PAA (covalently

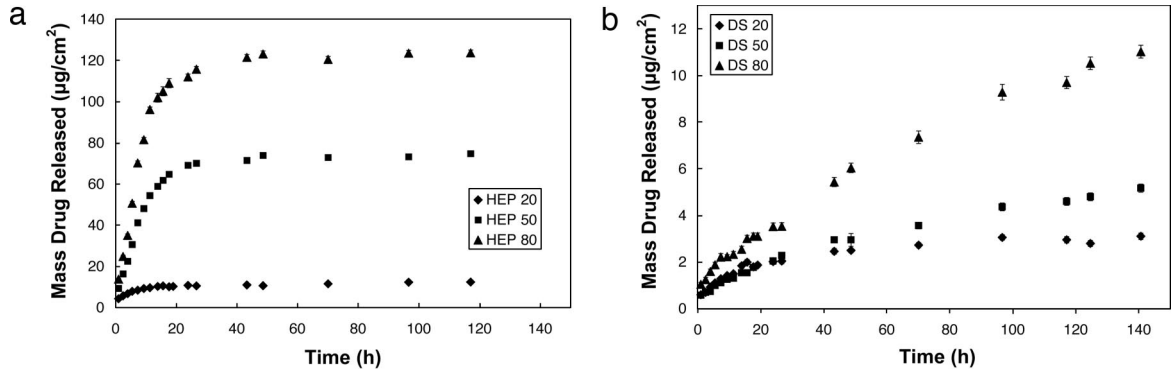

Fig. 3. Release from 20 (◆), 50 (■), and 80 (▲) bilayer films containing HEP (exponential) (*a*) and DS (linear) (*b*) with time (surface area normalized; error bars are small).

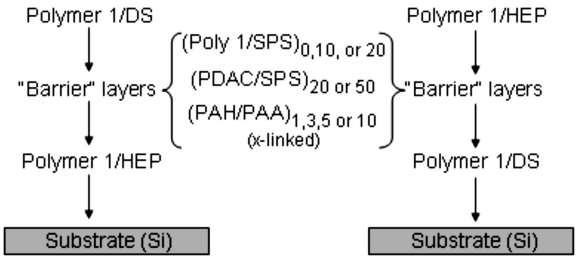

Fig. 4. Schematic depicting strategies employed in this study to construct physical barriers to control interlayer diffusion in multicomponent films.

crosslinked for 20 min at 215°C), followed by the deposition of polymer 1/HEP, we observed a multistage, serial release of first the surface HEP followed by the underlying DS. Thus, the use of a single covalently crosslinked PAH/PAA layer was sufficient to separate the two components when deposited onto the surface of the linearly growing polymer 1/DS system, as evidenced by the two-stage release profile. After the ≈25-h time delay, underlying DS was released with a linear profile. Interestingly, the average rate of DS release was ≈60% slower than that observed in corresponding films without covalently crosslinked barrier layers. Additional experiments using single and multiple crosslinked PAH/PAA barrier layers show that the duration of the release delay and the rate of release after this delay can be broadly controlled under this approach. For example, multiple layers of PAH/PAA crosslinked for longer than 1.5 h (at 215°C) virtually halted the release of all underlying DS (no release of DS was observed for up to 45 days). This result may have important and direct applications in drug delivery, because it suggests that both the timing and rate of release of an underlying species can be broadly controlled using as little as a single crosslinked bilayer. Interestingly, we also found that when the order of the two labeled components was reversed (HEP as the base layer and DS as the surface layer) it was no longer possible to achieve serial release of the two components using crosslinked spacer layers, suggesting that the nature of the base film onto which the crosslinked barrier layer is absorbed influences the final properties of the barrier layer (Fig. 8, which is published as supporting information on the PNAS web site).

Remarkably, all of the noncovalent (noncrosslinked) barrier layers designed to physically separate the HEP and DS systems (Fig. 4) resulted in simultaneous release of both components (see Figs. 9–14, which are published as supporting information on the PNAS web site). In most cases the barrier layers failed to even slow the release of the initially deposited base layers (Fig. 6). To further verify these findings, the above series of films was repeated at a range of fabrication conditions (pH, ionic strength, and number of deposited barrier layers), yet all resulted in simultaneous, rapid release in every case studied (data not shown). These data suggest that noncovalent, electrostatically assembled barrier layers cannot block interlayer diffusion and, therefore, cannot be used to create compartmentalized structures involving diffusive polyelectrolytes. This finding is particularly interesting in light of a recent study that showed that compartmentalized films containing linearly and exponentially growing regions could be constructed simply by depositing different films directly on top of one other (23). The incongruities between this study and ours could be a result of a number of factors, including different polymer systems, molecular weights, and deposition conditions; moreover, they suggest that factors outside of the nature of growth that a given system exhibits may powerfully influence the final film architecture.

To more clearly demonstrate the effect of barrier layers on the average release rate from the aforementioned two-component systems, release rate is normalized and charted versus the type of barrier layer used in Fig. 6. In Fig. 6*a*, it is apparent that the average release rate (taken as the average slope of the initial, linear portion of the release curve) of systems composed of an underlying layer of linearly growing DS can be broadly controlled by using both multiple layers of a nondegradable system PDAC/SPS or as little as a single layer of crosslinked PAH/PAA. Furthermore, by tuning any of the parameters affecting the degree of crosslinking (e.g., crosslinking time, temperature, or number of crosslinked layers), the release rate can be dramatically altered (crosslinking times of >1.5 h at 215°C and barriers containing more than five crosslinked layers, resulted in one- to two-order-of-magnitude decreases in release rate) (data not shown). Thus, milder crosslinking conditions (such as lower temperatures) may allow for a greater degree of flexibility in tailoring release profiles. Furthermore, aqueous, chemical crosslinking techniques using common biochemical reagents such as carbodiimides may represent a suitable alternative to thermal crosslinking when low temperature fabrication is required. Nevertheless, these proof-of-principle studies suggest that sampling a range of approaches to control the release of underlying species can yield effective results, particularly when the underlying species lacks the ability to diffuse throughout the film.

Taken together, the data in Figs. 5 and 6 yield a set of interesting hypotheses with respect to diffusion and release from multicomponent, hydrolytically degradable LbL films. First, when initially deposited layers contain a highly diffusible species, such as HEP, subsequent deposition of additional layers has little to no effect on its release because the diffusible species is likely able to migrate through tightly interacting networks within the

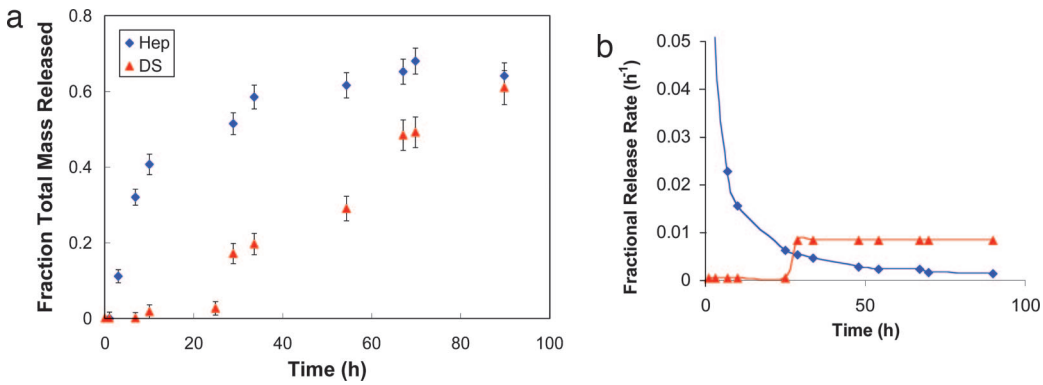

Fig. 5. DS (base layer, ▲) and HEP (surface layer, ◆)-loaded layers separated by a single, crosslinked layer of (PAH/PAA) exhibit sequential release. (*a*) Fraction of mass-released versus degradation time. (*b*) Fractional release rate versus time.

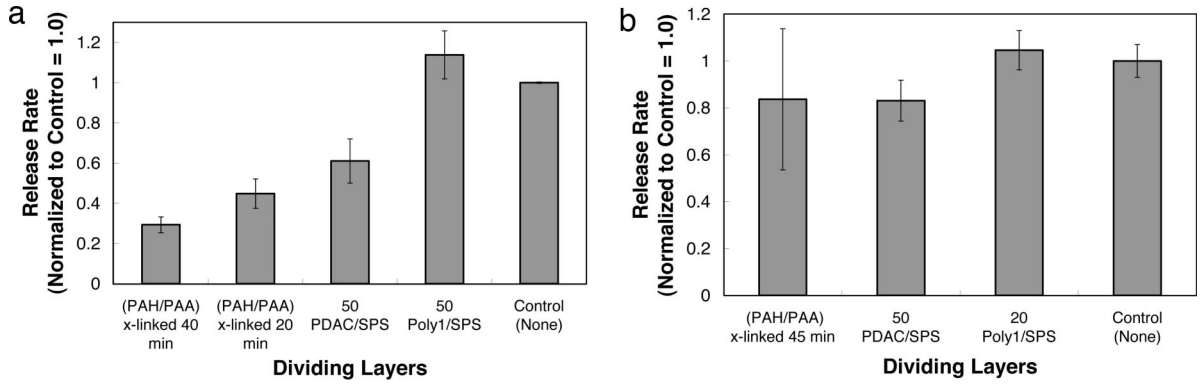

Fig. 6. Normalized initial average release rate (micrograms per hours per squared centimeter) from base films containing DS (*a*) and HEP (*b*) coated with no separation layers (control) or with a single layer of PAH/PAA crosslinked at 215°C for variable times, nondegradable PDAC/SPS, or degradable polymer 1/SPS. Initial average release rates were calculated from the average slope of the linear portion of the mass-released versus time curve during the first 50 h (DS) or 10 h (HEP) of degradation.

film, effectively ensuring that it always resides near the film surface (4). However, when initially deposited layers contain a linearly growing species, such as DS, subsequent deposition of new species can have a significant impact on its release because the linearly growing system provides a structural substratum on which a tightly interacting network of barrier layers can be formed (which can then serve to hinder its release during degradation by physically separating it from subsequently adsorbed species). We demonstrate that a relatively simple understanding of the nature of build up and diffusion within a given system can allow one to engineer stratified, multicompartment architectures with complex release profiles and that these profiles can be broadly controlled to suit the demands of a particular application.

Conclusions

In this work, we systematically probed a series of strategies designed to physically separate multiple components within a LbL film by blocking interlayer diffusion. We measured the effect of each type of barrier by using an experimental system consisting of a hydrolytically degradable polymer alternately deposited with a series of radiolabeled polyelectrolytes. With this approach, we uncovered a set of strategies that allow for the production of compartmentalized, or stratified, films capable of releasing complex, tuned release profiles. In particular, we show that covalently crosslinked barriers can effectively block interlayer diffusion, leading to compartmentalized structures, although even very large numbers of ionically crosslinked (degradable or nondegradable) barrier layers cannot block interlayer diffusion. Perhaps most interestingly, we demonstrate that wide-ranging materials properties can be obtained from a single, relatively simple set of materials by judiciously applying strategies to control interlayer diffusion. Combining the attributes of the LbL processing technique, which allows for the rapid, all-aqueous, conformal fabrication of nanoscale coatings that are highly uniform and tunable, with the ability to spatially order active agents and control release kinetics for multiple species may yield significant opportunities in drug delivery, separations, electrooptical materials, and other fields.

Materials and Methods

Materials. Polymer 1 [M_n = 10,000 (M_n is number-average molecular weight)] was synthesized as previously described (24). HEP sodium salt (M_n = 12,500) was obtained from Celsus Laboratories (Cincinnati). DS sodium salt (M_n = 8,000), poly(sodium 4-styrenesulfonate) (M_n = 1 million), PAH (M_n = 70,000), and PDAC (M_n = 100,000) were obtained from Sigma–Aldrich. Linear poly(ethylenimine) (M_n = 25,000) and PAA (M_n = 90,000) were purchased from Polysciences. Silicon wafers (test grade n-type) were purchased from Silicon Quest (Santa Clara, CA). [^{3}H]HEP sodium salt [1 mCi (1 Ci = 37 GBq), 0.30 mCi/mg, M_n = 12,500] and [^{14}C]DS sodium salt (100 μCi, 1.5 mCi/g, M_n = 8,000) were obtained from American Radiolabeled Chemicals (St. Louis). Radiolabeled and corresponding unlabeled polymers were chosen with similar molecular weights and polydispersities to mimic the behavior of the unlabeled species as closely as possible. All materials and solvents were used as received without further purification.

General Considerations. A Harrick PDC-32G plasma cleaner was used to etch silicon substrates (3 × 2 cm) after they were rinsed with methanol and deionized water and dried under a stream of dry nitrogen. LbL thin films were deposited with an automated Zeiss HMS-series programmable slide stainer. Absorbances from growing films were measured by FTIR with a Nicolet Magna IR 550 Series II spectrometer. Zinc selenide substrates used for transmission FTIR analysis were prepared by the same method used for silicon substrates. Ellipsometric measurements for film thickness were conducted by using a Gaertner variable angle ellipsometer (6,328 nm, 70° incident angle) and GEMP 1.2 (Gaertner Ellipsometer Measurement Program) software interface. The release of radiolabeled polymers was quantified by using a Tri-Carb liquid scintillation counter (model U2200, Packard). The amount of radiolabel in each sample vial was measured by using ^{3}H, ^{14}C, and dual counting protocols, each of which were shown to be both consistent and highly accurate over a broad concentration range (30–100,000 dpm/ml) in calibration experiments performed before drug release. Thermal crosslinking of PAH/PAA films was performed by incubating films in a Yamoto DVS400 gravity convection oven at 215°C for the time intervals indicated in Fig. 6.

Thin-Film Fabrication. All films were constructed from dilute aqueous solutions (2–10 mM) using the alternating dipping method (3). All polymers used in degradable thin films were prepared in 100 mM acetate buffer at pH 5.1 to avoid the conditions under which polymer 1 degrades rapidly ($t_{1/2} > 10$ h at pH 5.1 and 37°C) (24). Nondegradable base layers were deposited from dipping solutions of linear poly(ethylenimine) and poly(sodium 4-styrenesulfonate) in deionized water pH adjusted to 4.25 and 4.75, respectively. Deionized water used to prepare all solutions was obtained via a Milli-Q Plus (Millipore) at 18.2 MΩ. For degradation experiments, 1× PBS buffer (137 mM NaCl/2.7 mM KCl/10 mM Na_2HPO_4, pH 7.4) was used.

Films used in this study were constructed on either silicon (for ellipsometry and degradation studies) or zinc selenide (for transmission-mode FTIR) planar substrates. In all cases, degradable, polymer 1-based films were constructed directly on top of 10 bilayer, nondegradable base films containing linear poly(ethylenimine) and SPS to ensure uniform adhesion to the substrate. After deposition, films were removed from rinsing baths and dried thoroughly under a stream of dry nitrogen to avoid premature degradation.

Thin-Film Degradation Studies. All film degradation studies were performed as follows. Films were immersed in 20 ml of the appropriate buffer solution in a screw-top glass vial and tightly sealed. At designated times, films were removed and dried thoroughly under a stream of dry nitrogen, and thickness was measured using ellipsometry at 10 predetermined locations on the film surface (measurements were performed in triplicate). After the measurements were taken, the films were reimmersed in buffer solutions and resealed.

Release Studies. For drug-release experiments, radiolabeled LbL thin films were first constructed by alternately depositing polymer 1 and the indicated radiolabeled drug(s). Radiolabeled deposition solutions containing [^{3}H]HEP were prepared by combining 1 ml of 50 μCi/ml [^{3}H]HEP (0.30 mCi/mg, M_n = 12,500) with 35 ml of 100 mM acetate buffer. Unlabeled HEP (M_n = 12,500) was added to bring the total concentration of HEP (unlabeled plus labeled) to 2 mg/ml (1.5–2 μCi/ml ^{3}H). Radiolabeled deposition solutions containing [^{14}C]DS were similarly prepared by combining [^{14}C]DS (1.5 mCi/g, M_n = 8,000), unlabeled DS (M_n = 8,000), and 100 mM acetate buffer to yield a total concentration of DS (unlabeled plus labeled) to 2 mg/ml (1 μCi/ml ^{14}C). After fabrication of the indicated films, drug-release experiments were performed by immersing each film in 50 ml of 1× PBS buffer in a 200-ml screw-top vial. A 1-ml sample was extracted at the time points indicated in Figs. 2, 3, 5, and 8–14 and analyzed by adding 5 ml of ScintiSafe Plus 50% (Fisher Scientific) before measurement. Degradation vials were tightly capped between sample extractions to prevent evaporation of the buffer solution. Raw data (given in disintegrations per minute) were converted to micrograms of drug released using the conversion factor 2.2 × 10^6 DPM = 1 μCi, the specific radioactivity of the drug, and our knowledge of the ratio of total drug to labeled drug in the deposition solution (13).

We thank Yun Xie and Yamicia Connor for experimental assistance and Prof. Robert Langer (Massachusetts Institute of Technology) for helpful discussions and for the use of the scintillation counter in his laboratory. This work was supported by the Deshpande Center for Technological Innovation; Division of Materials Research/National Science Foundation Grant DMR 9903380; the Office of Naval Research; and the Mark Hyman, Jr., Professorship in Chemical Engineering at the Massachusetts Institute of Technology. H.F.C. is the recipient of a National Defense Science and Engineering Graduate Research Fellowship. R.D.B. thanks the Massachusetts Institute of Technology Undergraduate Research Opportunities Program for undergraduate research fellowships.

1. Hammond, P. (2004) *Adv. Mater.* **16,** 1271–1293.
2. Anderson, D., Burdick, J. & Langer, R. (2004) *Science* **305,** 1923–1924.
3. Decher, G. (1997) *Science* **277,** 1232–1237.
4. Picart, C., Mutterer, J., Richert, L., Luo, Y., Prestwich, G., Schaff, P., Voegel, J. & Lavalle, P. (2002) *Proc. Natl. Acad. Sci. USA* **99,** 12531–12535.
5. Hammond, P. (2000) *J. Colloid Interface Sci.* **4,** 430–432.
6. Caruso, F., Yang, W., Trau, D. & Renneberg, R. (2000) *Langmuir* **16,** 8932–8936.
7. Onda, M., Lvov, Y., Ariga, K. & Kunitake, T. (1996) *Biotechnol. Bioeng.* **51,** 163–167.
8. Lvov, Y., Ariga, K. & Kunitake, T. (1995) *J. Am. Chem. Soc.* **117,** 6117–6123.
9. Thierry, B., Winnik, F., Merhi, Y. & Tabrizian, M. (2003) *J. Am. Chem. Soc.* **125,** 7494–7495.
10. Jessel, N., Atalar, F., Lavalle, P., Mutterer, J., Decher, G., Schaff, P., Voegel, J. & Ogier, J. (2003) *Adv. Mater.* **15,** 692–695.
11. Vazquez, E., DeWitt, D., Hammond, P. & Lynn, D. (2002) *J. Am. Chem. Soc.* **124,** 13992–13993.
12. Zhang, J., Chua, L. & Lynn, D. (2004) *Langmuir* **20,** 8015–8021.
13. Wood, K., Boedicker, J., Lynn, D. & Hammond, P. (2005) *Langmuir* **21,** 1603–1609.
14. Jewell, C., Zhang, J., Fredin, N. & Lynn, D. (2005) *J. Controlled Release* **106,** 214–223.
15. Hübsch, E., Ball, V., Senger, B., Decher, G., Voegel, J. & Schaaf, P. (2004) *Langmuir* **20,** 1980–1985.
16. Lösche, M., Schmitt, J., Decher, G., Bouvman, W. & Kjaer, K. (1998) *Macromolecules* **31,** 8893–8906.
17. Elbert, D., Herbert, C. & Hubbell, J. (1999) *Langmuir* **15,** 5355–5362.
18. Picart, C., Lavalle, P., Hubert, P., Cuisinier, F., Decher, G., Schaff, P. & Voegel, J. (2001) *Langmuir* **17,** 7414–7424.
19. Lavalle, P., Gergely, C., Cuisinier, F., Decher, G., Schaff, P., Voegel, J. & Picart, C. (2002) *Macromolecules* **35,** 4458–4465.
20. Lavalle, P., Picart, C., Mutterer, J., Gergely, C., Reiss, H., Voegel, J., Senger, B. & Schaaf, P. (2004) *J. Phys. Chem. B.* **108,** 635–648.
21. Anderson, D. G., Lynn, D. M. & Langer, R. (2003) *Angew. Chem. Int. Ed.* **42,** 3153–3158.
22. Fredin, N., Zhang, J. & Lynn, D. (2005) *Langmuir* **21,** 5803–5811.
23. Garza, J., Schaaf, P., Muller, S., Ball, V., Stoltz, J., Voegel, J. & Lavalle, P. (2004) *Langmuir* **20,** 7298–7302.
24. Lynn, D. & Langer, R. (2000) *J. Am. Chem. Soc.* **122,** 10761–10768.